A mechanism for hopping magnetoresistance in antiferromagnetic insulators with application to La_2CuO_4

A. O. Gogolin

P. N. Lebedev Institute of Physics, USSR Academy of Sciences

A. S. Ioselevich

L. D. Landau Institute of Theoretical Physics, USSR Academy of Sciences

(Submitted 12 March 1990)
Zh. Eksp. Teor. Fiz. **98**, 681–702 (August 1990)

We propose a spin-dependent mechanism for hopping magnetoresistance in insulators with complex magnetic structures. The mechanism is based on spin splitting of impurity states in the molecular field, which leads to a difference in hopping probabilities with and without spin flip. This causes the resistance to depend on the magnitude and mutual orientation of the molecular fields acting on the impurity spins, where these molecular fields and their mutual orientations are controlled by an external magnetic field. This mechanism can be the source of nontrivial behavior of the magnetoresistance; in particular, the latter can be negative and undergo jumps or kinks at magnetic phase transitions. We develop this theory in detail for La_2CuO_4, and construct its magnetic phase diagram. The results of the experiments of Thio *et al.*[1,2] can be explained on the basis of the following assumptions. First, the symmetry of the impurity state admits only a molecular field originating from the antisymmetric part of the exchange. Specific models are investigated which satisfy this condition (e.g., holes localized on a single oxygen site). Second, a local enhancement of the rhombohedral character of the lattice arises near a localized hole, i.e., a polaron effect. In our view, the data of Refs. 1, 2 can be regarded as indirect confirmation of such an effect in La_2CuO_4; the existence of this effect is important in understanding the nature of the current carriers and superconductivity.

1. INTRODUCTION

The work reported here was initiated by experiments[1–3] on the hopping conductivity of La_2CuO_4 in a magnetic field. In these experiments, a negative magnetoresistance was observed, having singularities at temperatures where reorientation magnetic phase transitions induced by external fields occur (Fig. 1).

It is clear that the usual mechanisms,[4] which are related to the compression of impurity wave functions in a magnetic field and which lead to an exponential positive magnetoresistance, cannot explain such behavior.

In this paper we propose a different mechanism for the magnetoresistance, which is related to spin. It is based on the following picture: localized impurity states possess a nonzero spin, which interacts with the molecular fields arising from the magnetic environment, causing the impurity level to split. The molecular fields are oriented differently for different impurities. The total probability for a carrier to hop between two impurities is the sum of the probabilities for transitions between various components of their spin multiplets (Fig. 2).

At low temperatures the dominant transition is between the lowest sublevels; this transition is especially important in the presence of the polaron effect. If the orientations of the molecular fields at two impurities are parallel, then the hopping transition takes place with conservation of spin. Conversely, for antiparallel molecular fields it is necessary for the spin to flip during the transition. Obviously, the probability of a transition with spin flip is considerably smaller than without it; thus, it follows that the total probability of a transition depends strongly on the mutual orientations of the molecular fields. The role of the external magnetic field reduces to regulating these orientations; this is the only way that the magnetic field can affect the probability of the transitions and, consequently, the resistivity of the sample. If the reorientation takes place discontinuously (at a certain critical field), then the resistance also may undergo a discontinuity. Let us note that the effect of magnetic order on the probability of hopping in the absence of an external field has been studied previously within the context of polaron transport theory (see Ref. 5). The effect of the interaction of the carrier spins on the hopping conductivity in normal (nonmagnetic) semiconductors was discussed in Ref. 6.

What requirements should a material satisfy in order for it to support a spin mechanism for its magnetoresistance?

First of all, the material should be a ferromagnet of the type that permits a significant amount of reorientation of the sublattice moments in experimentally attainable fields (for example, a layered antiferromagnet).

Secondly, this material should be an insulator with im-

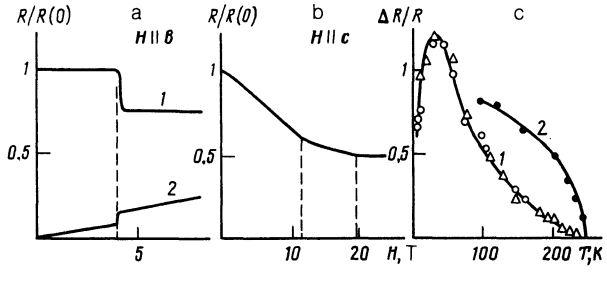

FIG. 1. Experimental data on the magnetoresistance of La_2CuO_4. a—dependence of the resistance (curve *1*) and total magnetic moment (curve *2*) on a field $\mathbf{H}\|\mathbf{b}$; b—the function $R(H)$ in a field $\mathbf{H}\|\mathbf{c}$; c—curve *1*—temperature dependence of the total variation of the resistance $[R(0) - R(\infty)]/R(\infty)$ for $\mathbf{H}\|\mathbf{b}$ (Δ) and $\mathbf{H}\|\mathbf{c}$ ($\bigcirc$); curve *2*—antiferromagnetic order parameter $M(T)$.

 0038-5646/90/080380-13$03.00 © 1990 American Institute of Physics

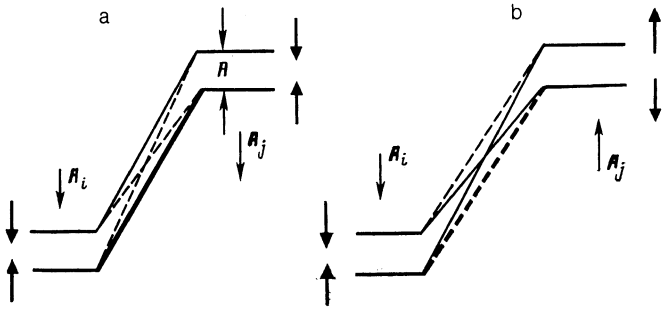

FIG. 2. Scheme for transitions between spin sublevels of acceptors i and j. The transitions with spin flip are shown by dashed lines, without spin flip by solid lines. The transition that dominates for $T \ll A$ is identified with boldface lines, a—the case $\mathbf{A}_i = \mathbf{A}_j$, b—$\mathbf{A}_i = -\mathbf{A}_j$.

purity hopping conductivity and localized states whose radius is small enough that the normal positive magnetoresistance should be small. This implies that the impurity state should be rather deep.

In addition to La_2CuO_4, which we will discuss below, there are other candidates for observing a nontrivial magnetoresistance, e.g., very pure single crystals of other complex magnets, in particular layered perovskites.

As far as we know, nontrivial behavior of the magnetoresistance in the hopping regime (Fig. 1) has been observed to date only in single-crystal La_2CuO_4. In addition, this material has been closely studied by investigators because it is one of the simplest of the high-temperature superconductors with regard to structure.[7,8] Therefore, we will attempt to tie our theory of spin magnetoresistance to the specific properties of La_2CuO_4.

Pure La_2CuO_4 (i.e., containing no more than 2–3% impurities) is a layered antiferromagnetic insulator.[8] A distinctive feature of its magnetic order is the fact that superimposed on the antiferromagnetically-ordered spins of the Cu^{2+} ions in the CuO_2 planes is a rotation of all the spins in a given plane by a rather small angle $\vartheta \approx 3 \cdot 10^{-3}$. This causes the planes to possess rather small ferromagnetic moments, which are ordered antiferromagnetically in the direction perpendicular to the planes.[1,9–12] The rotation of the spins is caused by the vector anisotropy of the Dzyaloshinskii–Moriya exchange interaction,[13–14] which in turn arises from a rhombohedral distortion of the lattice. Because the interplanar antiferromagnetic exchange is small, a transition occurs to a weakly ferromagnetic state in which the moments of the planes are parallel when even a weak field (~ 4 T) is applied perpendicular to the layers (i.e., $\mathbf{H} \| \mathbf{b}$, where $\mathbf{a}$, $\mathbf{b}$, and $\mathbf{c}$ are unit vectors in the rhombohedral system of axes).[1]

The insulator La_2CuO_4 is found to possess a resistance with Mott-like characteristics: $R(T) \propto \exp[(T_0/T)^{1/4}]$ (Ref. 15). In the purest samples, this dependence is replaced by a simple activated dependence at high temperatures, but the Mott law continues to hold for $T \lesssim 50$ K.[16] This implies that we are seeing three-dimensional variable-range hopping conductivity.[17] From this it follows that the charge carriers (holes in the CuO_2 planes) are localized within the impurity potential and the hopping takes place overwhelmingly between states on different planes.

Since the mechanism we are proposing for the magnetoresistance involves spin, it is very important to model the spin of the impurity state and the character of the molecular field acting on it. Let us first discuss the assumptions we will use in this paper regarding the structure of the impurity state.

1. The space group of symmetries of the impurity localized states contains an element which coincides with the operator that exchanges the magnetic copper sublattices in the CuO_2 planes.

This implies, first of all, that the spin S of the impurity state must be half-integral (for all the examples discussed in Sec. 3 $S = 1/2$ holds). Secondly, it implies that the molecular field equals zero within the isotropic-exchange approximation (i.e., it is forbidden by symmetry), and can be nonzero only by virtue of the rhombohedral symmetry which arises from the Dzyaloshinskii–Moriya interaction; if this is the case, then it is proportional to the magnitude of the rhombohedral distortion. Note that assumption number 1 is extremely important; in reality, if an exchange contribution were present in the molecular field, this field would be directed randomly (because of the random positions of the impurities relative to the sublattices). Therefore, reorientation of these fields could not change the resistance.

2. Localized holes cause a strong polaron effect which gives rise to a local enhancement of the rhombohedral distortion.

We argued in Ref. 18 that this effect should be present. It is important that in this case the rhombohedral distortion apparently must consist of two components: an enhancement of the weak uniform rhombohedral rotation around the a axis, which extends throughout the whole volume of the crystal, and a localized rotation around the c axis. Random fields acting between impurities and kinetic effects can lead to various types of order (or disorder) of this $\mathbf{c}$-component of the rhombohedral distortion. In this paper, we will discuss certain types of ordering in purely phenomenological terms without addressing the question of their physical origin from the standpoint of studying their effect on the hopping conductivity. From our viewpoint, assumption number 2 is necessary to explain the observed magnitude of the effect. Actually, if we assume that the rhombohedral distortion near an impurity is less than the rhombohedral distortion in the volume, then the jump in the resistivity is $\Delta R/R \propto \vartheta^2 \approx 10^{-5}$, which does not agree at all with the experiments, in which this jump is found to be ~ 1 (Figs. 1a, 1b). Note that the specific energy dependence of the transition probability which is inherent in polaron hopping also favors the spin mechanism for the magnetoresistance because it leads to a special role for transitions between low-lying sublevels of the spin multiplets.

In addition to the distortion of the lattice around a bound hole (i.e., a normal polaron) spin polarons, i.e., regions in which the magnetic order is disrupted, should appear in antiferromagnets. In the case of the CuO_2 planes, however, these polarons are not ferromagnetic Nagaoka polarons,[19] and do not tend to develop high spins (see Refs. 20, 21). These magnetic polarons do not affect the temperature and field dependences of the resistance, nor do they give rise to magnetic effects in tunneling (see Section 4), because the exchange is much larger than the temperatures and characteristic phonon frequencies.

The contents of this paper are organized as follows. In Sec. 2, we study the spin Hamiltonian of La_2CuO_4 in a magnetic field within the framework of mean-field theory, and

describe the possible magnetic phases and the sequence of phase transitions between them as the field increases (as a function of the parameters of the microscopic Hamiltonian). In Sec. 3 we discuss a specific model of impurity states. Sec. 4 is devoted to computing resistances that enter into a Miller–Abrahams network; the unusual percolation problem which arises in this case is solved in Sec. 5. In Sec. 6 we present the final expressions for the magnetoresistance and compare them with the experimental data.[1-3] In addition, we will discuss the possibility of experimental investigation of the structure of the impurity states.

2. MAGNETIC STRUCTURE OF La_2CuO_4 IN AN EXTERNAL FIELD

The interaction of two neighboring copper spins lying in the same CuO_2 plane has the form[1]

$$\mathcal{H}_{ij}=J\mathbf{S}_i\mathbf{S}_j+(\boldsymbol{\omega}_0[\mathbf{S}_i\mathbf{S}_j])+\Delta S_i^b S_j^b, \tag{1}$$

where J is the isotropic antiferromagnetic exchange, and $\boldsymbol{\omega}_0\|\mathbf{a}$ is the vector part of the anisotropic exchange, i.e., the Dzyaloshinskii–Moriya interaction,[13,14] which is a consequence of the rhombohedral distortion. The quantity $\omega_0\sim(\Delta g/g)Q_0J$, where $Q_0\approx 0.05$ is the angle of rotation of the oxygen octahedra in the rhombohedral phase, $\Delta g/g\approx 0.1$ (see Ref. 1). In the vector product, a spin that belongs to one of the two individual sublattices must always stand in the first position. The third term describes the easy-plane type of anisotropy ($\Delta>0$).

A primitive cell of La_2CuO_4 contains four copper atoms, therefore, it is a four-sublattice magnet. The averages of the sublattice moments we denote by $\mathbf{S}_{(+)\delta}$ and $\mathbf{S}_{(+)\varepsilon}$ for the other. In this paper we will assume from now on that the $\mathbf{S}_i$ are classical vectors ($|\mathbf{S}_i|=1/2$) and find the configuration of these vectors which corresponds to minimum energy:

$$\begin{aligned}E=z\sum_{\alpha=\pm}\{&J\mathbf{S}_{\alpha\varepsilon}\mathbf{S}_{\alpha\delta}+\boldsymbol{\omega}_0[\mathbf{S}_{\alpha\varepsilon}\mathbf{S}_{\alpha\delta}]+\Delta S_{\alpha\varepsilon}{}^bS_{\alpha\delta}{}^b\}+z'J_{\perp 1}(\mathbf{S}_{(+)\varepsilon}\mathbf{S}_{(-)\varepsilon}\\&+\mathbf{S}_{(+)\delta}\mathbf{S}_{(-)\delta})+z'J_{\perp 2}(\mathbf{S}_{(+)\varepsilon}\mathbf{S}_{(-)\delta}\\&+\mathbf{S}_{(+)\delta}\mathbf{S}_{(-)\varepsilon})-g\mu_B\sum_{\alpha=\pm}\mathbf{H}(\mathbf{S}_{\alpha\varepsilon}+\mathbf{S}_{\alpha\delta}),\end{aligned} \tag{2}$$

where $z=4$, $z'=2$ are the coordination numbers and $\mathbf{H}$ is the magnetic field. The interplanar exchange constants $J_{\perp 1}$ and $J_{\perp 2}$ differ with the amount of rhombohedral distortion, and their difference $J_{\perp 1}-J_{\perp 2}=J_\perp\sim Q_0^2J_{\perp 1}$ is the effective interplanar antiferromagnetic exchange.

Following Refs. 1 and 2, we introduce the vectors $\mathbf{F}_\alpha=\mathbf{S}_{\alpha\varepsilon}+\mathbf{S}_{\alpha\delta}$, which are the ferromagnetic moments, and $\mathbf{M}_\alpha=\mathbf{S}_{\alpha\varepsilon}-\mathbf{S}_{\alpha\delta}$, which are the antiferromagnetism vectors (i.e., staggered magnetizations) of the planes. Minimizing expression (2) with respect to the ferromagnetic moments $\mathbf{F}_\alpha$, we obtain (to within a constant term):

$$\begin{aligned}E=(1/2J)\sum_\alpha\{&(\boldsymbol{\omega}_0\mathbf{M}_\alpha)^2+2\Delta J(\mathbf{b}\mathbf{M}_\alpha)^2+{}^1/_4(g\mu_B)^2(\mathbf{H}\mathbf{M}_\alpha)^2\\&+g\mu_B[\mathbf{H}\boldsymbol{\omega}_0]\mathbf{M}_\alpha\}\\&+J_\perp\mathbf{M}_{(+)}\mathbf{M}_{(-)}-(g\mu_B\mathbf{H})^2/4J,\end{aligned} \tag{3}$$

$$\mathbf{F}_\alpha=(1/2J)[\mathbf{M}_\alpha\boldsymbol{\omega}_0]+(g\mu_B/4J)[\mathbf{H}-\mathbf{M}_\alpha(\mathbf{H}\mathbf{M}_\alpha)]. \tag{4}$$

In Eq. (3) we have taken terms of first order in Δ and J and second order in ω_0 and H. In this approximation we have $|\mathbf{M}_\alpha|=1$. In addition, we have neglected terms $\sim(J_{\perp 1}\omega_0^2/J^2)\mathbf{M}_{(+)}\mathbf{M}_{(-)}$ which contain terms of higher order in the spin-orbit coupling $(\Delta g/g)^2$, compared to $J_\perp$.

In the absence of an external field we have $\mathbf{M}_{(+)}=-\mathbf{M}_{(-)}\|\mathbf{c}$ while $\mathbf{F}_{(+)}=-\mathbf{F}_{(-)}=(1/2J)[\boldsymbol{\omega}_0\mathbf{M}_{(-)}]\|\mathbf{b}$. Thus, each plane has a weak magnetic moment but the total moment is zero because the moments of the planes alternate antiferromagnetically along the **b** axis (latent ferromagnetism).

In a sufficiently strong magnetic field, the system enters a state for which the ferromagnetic moments $\mathbf{F}_\alpha$ are directed along the field for all the planes. On the way to this state the system can pass through a number of intermediate magnetic phases, depending on the parameters entering into Eq. (3), which correspond to various extrema of the energy. Those that are of interest to us are listed in the table, where we have used the spherical coordinates $M_\alpha^a=\cos\xi_\alpha\sin\phi_\alpha$, $M_\alpha^b=\sin\xi_\alpha$, and $M_\alpha^c=\cos\xi_\alpha\cos\phi_\alpha$, and we have introduced the dimensionless parameters

$$I=\frac{J_\perp J}{\omega_0{}^2},\quad D=\frac{2\Delta J}{\omega_0{}^2},\quad h=\frac{g\mu_BH}{\omega_0},\quad \varepsilon=\frac{JE}{\omega_0{}^2}. \tag{5}$$

We refer to the state that minimizes the energy for $H=0$ (see Fig. 3a) as "antiferromagnetic." For $\mathbf{H}\|\mathbf{a}$ this state remains the ground state for any value of field. The ferromagnetic vectors $\mathbf{F}_\alpha$ contain a contribution which is linear in the field [the second term in Eq. (4)], corresponding to a susceptibility $\chi=1/2J$; phase transitions are absent in this orientation of the field. For the other orientations ($\mathbf{H}\|\mathbf{b}$ or $\mathbf{H}\|\mathbf{c}$), large fields give rise to a "ferromagnetic" state F^b or $\mathbf{F}^c$ (Figs. 3c, 3d). The possible intermediate phases are illustrated in Figs. 3b, 3e, 3f, 3g, 3h. We can observe two types of spin–flop phase SF_1 and SF_2. For $\mathbf{H}\|\mathbf{c}$ these phases were found in Ref. 11 from symmetry considerations. In the phases $SF_1^{b,c}$ there is a net loss in the Dzyaloshinskii invariant (compared to the phases $SF_1^{b,c}$ and $SF_2^{b,c}$); however, there is a gain in the magnetic energy which is larger than it is in $SF_2^{b,c}$.

Figure 4 shows the succession of magnetic transitions as the field increases as a function of the parameters I and D. The transition from the SF phase to the F phase is always continuous (i.e., without a jump in the magnetization). Naturally, the SF_2^c phase (Fig. 3h) coincides with the original AF^b phase (Fig. 3a) for $H=0$. The remaining transitions take place with jumps in the magnetization.

In Ref. 2, the phase transition sequences $AF^b\to F^b$ for $\mathbf{H}\|\mathbf{b}$ and $SF_2^c\to SF_1^c\to F^c$ for $\mathbf{H}\|\mathbf{c}$ were studied using Eq. (2). According to the estimates of Ref. 2 we have $I=0.5$, $D=1.5\pm 1$ (see Fig. 4); these numbers imply that the point on the phase diagram corresponding to the samples investigated in Refs. 1,2 is in fact located in the correct region for these sequences of transitions. In later sections, we will investigate only these specific sequences. It is noteworthy, however, that according to the data of Ref. 2 there is no jump in the magnetization for the transition $SF_2^c\to SF_1^c$, while jumps corresponding to the transition $AF^b\to F^b$ are clearly visible over a wide range of temperatures.[1] The absence of a jump for the transition $SF_2^c\to SF_1^c$ contradicts the predictions of theory. It is possible that the transition could correspond to the continuous transition $SF_2^c\to F^c$ instead; how-

TABLE I.

	H‖b	H‖c
AF	$\xi_{(+)} = \xi_{(-)} = 0,$ $\varphi_{(+)} = 0,\ \varphi_{(-)} = \pi,$ $\varepsilon = -I - h^2$	$\xi_{(+)} = -\xi_{(-)} = \pi/2,$ $\varphi_{(+)} = \varphi_{(-)} = 0,$ $\varepsilon = D - I - h^2$
SF_1	$\xi_{(+)} = \xi_{(-)} = 0$ $\cos\varphi_{(+)} = h/(2I-1),$ $\varphi_{(-)} = -\varphi_{(+)},$ $\varepsilon = 1 - I - h^2\frac{2I}{2I-1}$	$\sin\xi_{(+)} = -h/(2I+D-1),$ $\xi_{(-)} = \xi_{(+)},$ $\varphi_{(+)} = \pi/2,\ \varphi_{(-)} = -\pi/2,$ $\varepsilon = 1 - I - h^2\frac{2I+D}{2I+D-1}$
SF_2	$\cos\xi_{(+)} = h/(2I-D-h^2),$ $\xi_{(-)} = -\xi_{(+)},$ $\varphi_{(+)} = \varphi_{(-)} = 0,$ $\varepsilon = D - I - h^2/(2I-D-h^2)$	$\sin\xi_{(+)} = -h/(2I+D-h^2),$ $\xi_{(-)} = \xi_{(+)}$ $\varphi_{(+)} = 0,\ \varphi_{(-)} = \pi,$ $\varepsilon = -I - h^2/(2I+D-h^2)$
F	$\xi_{(+)} = \xi_{(-)} = 0,$ $\varphi_{(+)} = \varphi_{(-)} = 0,$ $\varepsilon = I - h^2 - 2h$	$\xi_{(+)} = \xi_{(-)} = \pi/2,$ $\varphi_{(+)} = \varphi_{(-)} = 0,$ $\varepsilon = I + D - h^2 - 2h$

ever, if this is the case, as the field **H**‖**c** increases only one phase transition should be observed (Fig. 4b). Additional experimental investigations to resolve this contradiction would be desirable.

Furthermore, the effective values of I and D (i.e., the position of the point on the phase diagram) ought to depend on the temperature and concentration of impurities (for example, in Ref. 12, which dealt with strongly-doped crystals, a jump was observed in the magnetization for **H**‖**c** which was not observed for **H**‖**b**). Therefore, generally speaking, we should expect to observe different sequences of phase transitions in various experiments.

3. IMPURITY STATES, VIBRONIC EFFECTS AND MOLECULAR FIELDS

The experiments described in Refs. 1, 2, 9, 16 were carried out using single crystal La_2CuO_4 with a rather small oxygen excess (i.e., $y > 0$). In Ref. 16 arguments were advanced to suggest that phase separation (i.e., an inhomogeneous distribution of the oxygen excess) occurs for $y > 1$–1.5%, while for $y < 1$–1.5% the distribution of oxygen is uniform. The Néel temperature T_N fails rapidly as y increases.[18,22] The high values of T_N for the samples whose magnetoresistance was measured in Refs. 1, 2 allow us to

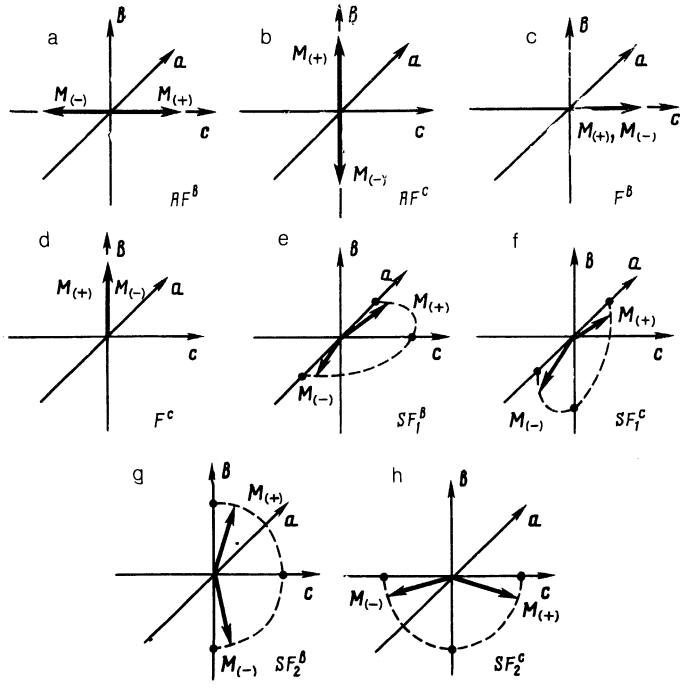

FIG. 3. Configuration of the antiferromagnetism vectors $\mathbf{M}_{(+)}$, $\mathbf{M}_{(-)}$ in neighboring planes which correspond to extrema of the energy (3) in a field **H**‖**b** (a,c,e,g) and in a field **H**‖**c** (b,d,f,h).

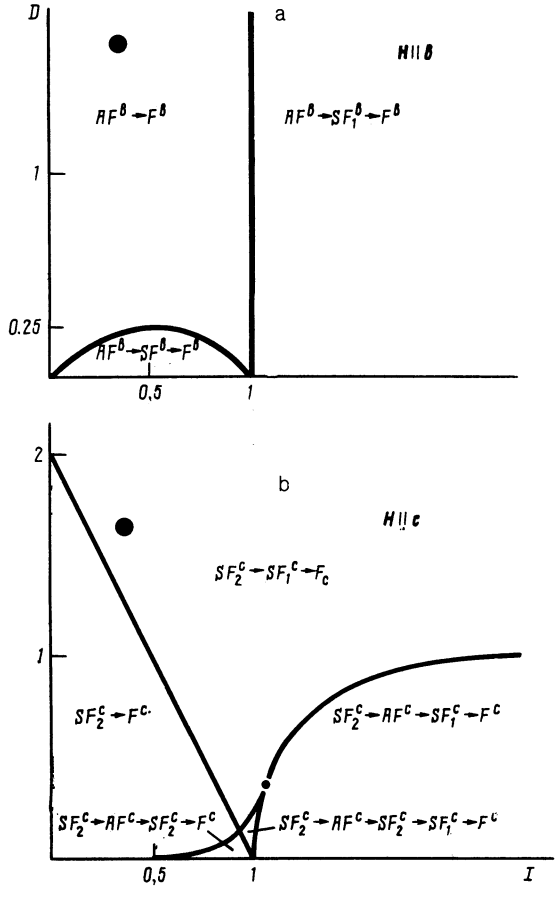

FIG. 4. Phase diagram in the I–D parameter plane [see Eq. (5)]. Shown here is the succession of magnetic phase changes as the field increases. a—**H**||**b**, b—**H**||**c**. ● is the point corresponding to the parameters of Ref. 2.

assert that in these samples the corresponding values of y were small and that the distribution of oxygen was homogeneous. The signs of the Hall coefficient and the thermoelectric power indicate that the additional oxygen atoms play the role of acceptors. The location of the additional oxygen in the lattice has not been established unambiguously. Possibly, the oxygen atoms are grouped as molecular O_2^- ions.[23]

At low temperatures ($T \lesssim 50$ K) the holes are bound to their acceptors, as indicated by the hopping nature of the conductivity.[15,16] According to various estimates,[15,24] the radius of the bound state (~ 10 Å) is comparable to the lattice period. In this intermediate situation, determination of the structure of the impurity state is not possible. However, a model of the deep impurity in which a hole is localized on the minimum number of oxygen sites among the nearest neighbors of the impurity is apparently a good approximation.[18,20,25]

In what follows, we will classify the possible types of deep neutral acceptors and identify one of them that satisfies requirements 1 and 2 formulated in the introduction.

If we assume that the motion of holes along the CuO_2 planes satisfies the Emery model[26] with a large Coulomb repulsion at the copper sites, then the Hamiltonian for the system of holes in the impurity potential V_1 and Cu spins has the form

$$\mathcal{H}=\mathcal{H}_s+\mathcal{H}_h, \tag{6}$$

where $\mathcal{H}_s = \Sigma_{ij}\mathcal{H}_{ij}$ [see Eq. (1) and Refs. 21, 27], and

$$\mathcal{H}_{hl}=t\sum_{\langle ill'\rangle} a_{l'}^{+}\hat{P}^i a_l+\tau\sum_{\langle il\rangle} a_l^{+}\hat{P}^i a_l+\sum_l V_l a_l^{+}a_l, \tag{7}$$

where a_l^+ and a_l are hole operators and $\hat{P}^i$ is the Dirac operator which interchanges the position of a hole spin and the spin of the i-th copper atom. The subscript l labels the oxygen atoms while i labels the copper atoms; $\langle ill'\rangle$ is a triplet made up of the ith copper and the two neighboring oxygen atoms ($l \neq l'$); t is the amplitude of a process in which a hole first passes from the copper atom i to oxygen atom l', followed by a hole hopping from oxygen atom l to copper atom i; τ is the same amplitude for the case $l = l'$ (we have $\tau < t$ because of the Coulomb repulsion at the oxygen site). In the deep impurity model $|V_1 - V_2| \gg t$, where $V_{1,2}$ are potentials at oxygen sites that are nearest neighbors (i.e., belonging to the first shell) and next-nearest-neighbors to the impurity; this implies that the motion of a hole will be limited to the first shell. Possible geometries of these localized states are shown in Fig. 5. The amplitudes satisfy $t, \tau \gg J$ (see Refs. 21, 27); therefore, the spins of the Cu^{2+} ions adjacent to the first shell interact with the hole much more strongly than they do with the spins of the magnetic subsystem. This allows us to isolate a cluster made up of a finite number of copper and oxygen atoms and find the spectrum of states of this cluster exactly.

In the simplest case, there is only one oxygen site close to the acceptor. The first shell consists of this site alone, and the cluster is shown in Fig. 5a. The ground state of the cluster corresponds to a total spin $S = 1/2$ (Ref. 20).

The cluster that corresponds to two oxygen sites neighboring the acceptor is shown in Fig. 3b. The spin of its ground state is $S = 0$; it is easy to verify this by direct calculation. We note that this result also follows from a rigorous theorem of Lieb and Mattis,[28] because the cluster in Fig. 5b is one-dimensional. There exists two situations in which there are four oxygen sites neighboring the acceptor. The cluster (Fig. 5c) was studied in Ref. 25; its ground state has spin $S = 0$. The cluster (Fig. 5d) was studied in Refs. 18, 25 (in an investigation of the structure of the ground state of a hole bound to the impurity ion Sr^{2+}). The ground state has spin $S = 1/2$ and is doubly orbitally degenerate, because it transforms according to the E representation of the point symmetry group C_{4v}. The clusters (Figs. 5b, 5c) do not satisfy requirement 1; therefore, in what follows they will not be considered.

We note that in all the cluster calculations (at least those for which $t = \tau$) the spin of the system ground state (i.e., hole + copper spins) was found to be as small as possible; zero for an odd number of copper ions in the cluster, and 1/2 for an even number. In this regard, the Emery model differs in an important way from the magnetic semiconductor[29] and the Hubbard[19] models, in which a magnetic polaron forms with maximum spin. We believe that within the Emery model (for which $ct = \tau$ holds) the assertion that the spin is a minimum is valid for any cluster. For an infinite cluster this hypothesis was formulated in Ref. 21. A rigorous proof of this has not been carried out up to now; it has only been shown that the magnetic polaron is unsaturated in all cases.

Up to now we have considered methods of localizing a hole within one plane. However, it is possible to have an acceptor positioned symmetrically between two neighboring

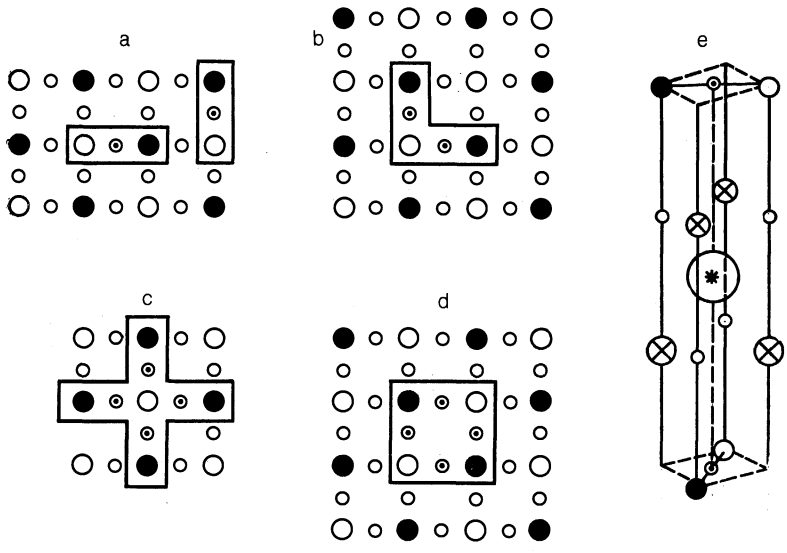

FIG. 5. Various types of localization of holes, ○,● are copper ions (the large circles) belonging to the different magnetic sublattices, ⊙ are oxygen sites (the small circles) from the first shell, ○ are the remaining oxygen sites, ⊗ are the La^{3+} ions, and ⊛ is the impurity ion. The cluster is bounded by the solid lines; a–d are configurations embedded in a single CuO_2 plane, e is a two-plane configuration.

planes (see Fig. 5b), in which the first shell consists of two oxygen sites from the neighboring planes. Because this cluster contains an even number of copper ions (4), the spin of the ground state is half-integral, i.e., $S \neq 0$.

The classification described above of the states of the system applies to a rigid lattice. However, in the perovskites, to which class La_2CuO_4 belongs, it often turns out that the vibronic interaction is important, leading to polaron effects.[30] In La_2CuO_4 the rhombohedral Σ_4 mode, which is responsible for the structural phase transition, remains soft over a wide interval of temperatures.[8,31] This is a doubly-degenerate mode (Q_1, Q_2), corresponding to alternating rotations of the oxygen octahedra relative to the **a** and **c** axes, respectively. Apparently, it is this mode in particular that is of primary importance in creating the local deformation near the impurity.

Let us first assume the hole is localized on a single site (Fig. 5a). In this case there are two local normal modes of type $Q_1 \pm Q_2$, which are constructed out of the soft rhombohedral mode. Both of these are odd relative to reflection in the CuO_2 plane and are coupled to the hole by the squared vibronic interaction. Only one of the normal modes couples the oxygen atom on which the hole is localized to the distortion. The vibronic interaction with this mode can be strong and cause a local deformation of the lattice.

Vibronic effects for the case of an acceptor whose symmetry corresponds to the cluster (Fig. 5d) were investigated in detail in Ref. 18. A degenerate local mode of type $Q_{1,2}$ mixes the ground and lowest excited states (the pseudo-Jahn–Teller effect). In this case two configurations are possible: either a "two-component" configuration, in which the energy minimum corresponds to $|Q_1| = |Q_2| \neq 0$, or a "single-component" configuration with $Q_1 \neq 0$, $Q_2 = 0$. In the first case, the hole is primarily found on one oxygen site; in the second case, it is primarily found on two.

It is also possible to have a local enhancement of the rhombohedral distortion in the two-plane configuration (Fig. 5e). In this case, the symmetry between planes can be spontaneously broken as a consequence of the pseudo-Jahn–Teller effect if the tunneling integral t' is not too large (i.e., if it does not exceed the polaron shift). This situation corresponds once more to the single-oxygen case (Fig. 5a). If, however, t' is large, then the symmetry between the planes can be preserved.

If the vibronic interaction is very strong, then a small-radius polaron forms, i.e., the hole is localized on a single site. Then all the other cases (Figs. 5b, 5c, 5d, 5e) become effectively equivalent to Fig. 5a. Furthermore, when the polaron effect is strong, the position of the acceptor in the lattice (i.e., the impurity potential) is actually not very important; its primary function is to determine the site at which the polaron is localized.

Therefore, in all the cases treated here, the vibronic interaction can enhance the rhombohedral distortion locally,[18] while the small overall rhombohedral distortion acts to stabilize the sign of the Q_1-component of the local distortion. In the case of a hole localized on a single site, the sign of the Q_2-component is strictly correlated with the sign of Q_1, although it also depends on the position of the cluster in the lattice. For localization on a plaquette (Fig. 5d), the sign of Q_2 is not stabilized by the uniform rhombohedral distortion in the two-component configuration.

We have shown that for the deep-impurity case (but even for the case of a shallow impurity when the polaron effect is strong) there exists a well-defined cluster made up of a certain number of copper spins that interact with the hole, which is localized within the first shell. The strong interaction of the copper spins with the hole forms a state of the cluster characterized by a total spin S. The influence of the antiferromagnetic neighborhood on the cluster is relatively weak, so that the internal structure of the latter is not disrupted and the interaction reduces to a coupling of the lattice with the total spin. This implies that singlet clusters (Figs. 5b, 5c) do not interact with the environment (for this reason we have not discussed them here), while for clusters with $S = 1/2$ (Figs. 5a, 5d) the symmetry admits only interactions of the form

$$\mathcal{H}_i = \mathbf{S}_i \mathbf{A}_i, \tag{8}$$

$$\mathbf{A}_i = J_i \mathbf{n}_i + [\mathbf{n}_i \boldsymbol{\omega}_i], \tag{9}$$

where $\mathbf{n}_i$ is the antiferromagnetism vector near the i-th acceptor. In general, the molecular field $\mathbf{A}_i$ contains two contributions. The first is the usual exchange contribution ($J_i \sim J$), while the second arises from the Dzyaloshinskii–

Moriya interaction. For an undeformed cluster (Figs. 5a, 5d), the exchange contribution is absent because there exists an element of the spatial symmetry of the copper lattice which is equivalent to interchanging the magnetic sublattices, i.e., it satisfies requirement 1. For the case of localization at a single oxygen site this symmetry is preserved even in the presence of vibronic effects, and again the exchange field does not appear. All this is true for the two-component localization configuration on a plaquette as well (Fig. 5d). In the single-component configuration the vibronic effect breaks the symmetry relative to the interchange of sublattices, leading to the appearance of an exchange field.

In Eq. (9) ω_i is the vector of the local rhombohedral distortion; hence

$$\omega_i \sim J(\Delta g/g)\,(Q_{1i}, Q_{2i}).$$

The quantity ω_i may differ significantly from the uniform rhombohedral distortion ω_0, if the local enhancement makes $Q_i \gg Q_0 \approx 0.05$; in this case ω_i reaches a value ~ 100–200 for $Q_i \sim 1$.

Thus, in the most important cases (Fig. 5d for the two-component configuration, and Figs. 5a, 5e), assertions 1 and 2 concerning the structure of acceptors are fulfilled (i.e., the polaron effect is strong). Therefore, a hole localized on these acceptors forms a "magnetic impurity" with spin $S = 1/2$, which is subject to a molecular field arising from the antiferromagnetic host of the form

$$\mathbf{A}_i = [\mathbf{n}_i \boldsymbol{\omega}_i], \tag{10}$$

This field does not contain the exchange contribution, and

$$\boldsymbol{\omega}_i = \omega(\mathbf{a} + \nu_i \mathbf{c}), \tag{11}$$

where $\nu_i = \pm 1$. For the configuration shown in Fig. 5e, see Eq. (12).

For the case of localization at a single site, each acceptor is characterized by a definite value of ν_i, which does not fluctuate with time; this quantity depends on the position of a given oxygen site in the lattice (i.e., on whether it is found on a horizontal or a vertical bond, see Fig. 5a). If the distribution of acceptors on the bonds is random, then the value of ν_i is also random. We will refer to this situation as "frozen-in disorder." Another situation may present itself, in which the values of ν_i are strongly correlated because of certain cooperative effects. For example, if all the acceptors are located on the horizontal (vertical) bonds, then we have $\nu_i = 1$ ($\nu_i = -1$). This case we will refer to as "uniform order." Also possible are orderings of the type $\nu_i = \alpha_i$ ("alternating order").

For the case of localization on a plaquette, in addition to the possibilities listed above (i.e., order and frozen-in disorder), a situation can arise in which ν_i for each acceptor fluctuates rapidly with time. In this latter case we will speak of "dynamic disorder."

For the two-plane configuration (Fig. 5e), the exchange contribution to the molecular field is again absent, and Eq. (10) converts to the form

$$\mathbf{A}_i = \omega\{[(\mathbf{n}_i^{(+)} + \mathbf{n}_i^{(-)})\mathbf{a}] + \nu_i[(\mathbf{n}_i^{(+)} - \mathbf{n}_i^{(-)})\mathbf{c}]\}, \tag{12}$$

where $\mathbf{n}^{(\pm)}$ are the antiferromagnetism vectors above and below the i-th acceptor, respectively. The two-plane configuration will not be treated in detail here because it is highly unlikely that an enhancement of the rhombohedral distortion will not be accompanied by breaking of the symmetry between the planes; furthermore, as we will show in Section 6, this configuration would correspond to an incorrect variation of the resistance in the field $\mathbf{H} \| \mathbf{b}$.

4. THE MILLER–ABRAHAMS RESISTIVE NETWORK

The theory of hopping conductivity given in Ref. 4 is based on a representation consisting of a network of random resistors

$$R_{ij} = T/e^2 \Gamma_{ij}.$$

Here Γ_{ij} is the average number of transitions between acceptors i and j:

$$\Gamma_{ij} = \langle p_i(1-p_j) W_{ij}(\mathbf{A}_i, \mathbf{A}_j) \rangle_t, \tag{13}$$

where p_j is the occupation number and W_{ij} is the hole transition probability from an occupied acceptor i to an empty one j.

In carrying out the time average in Eq. (13), we use a hierarchy of characteristic time scales. Estimates show that

$$\tau_s \ll \tau_n \ll \tau_\nu, \ \tau_0, \tag{14}$$

where τ_0 is the exponentially-large lifetime of a hole on an acceptor; within this time a Fermi function distribution $\langle p_i \rangle = f(\varepsilon_i)$ is established; ε_i is the hole energy on the i-th acceptor measured from the chemical potential; τ_ν is a characteristic fluctuation time of ν_i ($\tau_\nu < \infty$ only in the case of dynamic disorder); $\tau_n \sim 10^{-12}$ sec is a characteristic fluctuation time for the antiferromagnetism vector $\mathbf{n}$; $\tau_s \sim 10^{-13}$ sec is the relaxation time of the impurity spin. The right-hand inequality (14) allows us to write Eq. (13) in the form

$$\Gamma_{ij} = f(\varepsilon_i)\,[1 - f(\varepsilon_j)]\,\langle W_{ij}(\mathbf{A}_i, \mathbf{A}_j) \rangle_t. \tag{15}$$

At the same time, the left side (14) allows us to introduce the instantaneous quasiequilibrium distribution function of the impurity spin

$$F(\sigma_i) = \exp(-A_i\sigma_i/T)/2\,\mathrm{ch}\,(A_i/2T), \tag{16}$$

where we have written $A_i = |\mathbf{A}_i|$, and $\sigma_i = \pm 1/2$ are the projections of the impurity spin $\mathbf{S}_i$ onto the instantaneous direction of the molecular field $\mathbf{A}_i$. Then we obtain for the transition probability

$$W_{ij}(\mathbf{A}_i, \mathbf{A}_j) = \sum_{\sigma_i \sigma_j} F(\sigma_i)\{\delta_{\sigma_i \sigma_j}[W_{ij}^0(\Delta_{ij}^{\sigma_i\sigma_j})\cos^2(\chi_{ij}/2) + W_{ij}^1(\Delta_{ij}^{\sigma_i\sigma_j})\sin^2(\chi_{ij}/2)] + \delta_{\sigma_i, -\sigma_j}[W_{ij}^1(\Delta_{ij}^{\sigma_i\sigma_j}) \times \cos^2(\chi_{ij}/2) + W_{ij}^0(\Delta_{ij}^{\sigma_i\sigma_j})\sin^2(\chi_{ij}/2)]\}, \tag{17}$$

where χ_{ij} is the angle between $\mathbf{A}_i$ and $\mathbf{A}_j$; the energy difference

$$\Delta_{ij}^{\sigma_i\sigma_j} = \varepsilon_j + A_j\sigma_j - \varepsilon_i - A_i\sigma_i, \tag{18}$$

while W^1, W^0 are the probabilities for transitions with and without spin flip. Equation (17) is obviously valid if we assume that the hole does not interact with the antiferromagnetic matrix along the tunneling path. However, it also remains valid when the interaction [of the form (7)] with a magnetic subsystem is strong, if we assume the quantity $\mathbf{n}$ is constant along the tunneling path. The dependence of W^0

and W^1 on the mutual positions of the acceptors is the same; in the exponential approximation it has the form

$$W_{ij}^{0,1} \propto \exp\{-\xi^{sp}(\mathbf{r}_{ij})\}. \tag{19}$$

This factor is the overlap integral of the hole wave functions at impurities i and j. If the motion of the hole through the barrier can be described within the framework of effective mass theory (i.e., $t/V \gg 1$, or a shallow impurity), then

$$\xi^{sp}(\mathbf{r}_{ij}) = 2[(r_a^2+r_c^2)/a_\parallel^2 + r_b^2/a_\perp^2]^{1/2}$$

(see, e.g., Ref. 4). For a deep impurity

$$\xi^{sp}(\mathbf{r}_{ij}) = 2(r_a+r_c)/a_\parallel + 2r_b/a_\perp.$$

The quantities $a_\parallel$ and $a_\perp$ are effective radii of the localized state in the CuO_2 planes and perpendicular to it. The interaction of a hole with the antiferromagnetic background during the hopping process does not change the functional dependence of $\xi^{sp}(\mathbf{r})$. Thus, in the case of a deep impurity, a hole retains the character of a virtual "string" of broken antiferromagnetic bonds which are re-established by the exchange interaction. The corresponding matrix elements depend exponentially on the length of the string, leading to renormalization (i.e., a decrease) of the radius of the state.

The local enhancement of the rhombohedral distortion gives the hopping a polaronic character. Because the rhombohedral distortion is locally enhanced near an occupied acceptor, while an empty acceptor causes no enhancement, standard calculation schemes can be applied,[17,32] leading to an energy dependence of the probability for polaron hopping of the form

$$W^{0,1}(\Delta) \propto \exp\{-(\lambda|\Delta|+\Delta)/2T\}, \tag{20}$$

where

$$\lambda = \begin{cases} 1-T/T^*, & T<T^*, \\ 0, & T>T^*, \end{cases} \qquad T^* = \frac{\hbar\Omega}{2\ln(W_p/\Delta)}, \tag{21}$$

here Ω is the frequency of the local mode ($\hbar\Omega \sim 100$ K, see Ref. 18), W_p is the polaron shift, and the quantity Δ equals the characteristic width of the Mott band.[4,17] The probabilities W^0 and W_1 have an overall exponential dependence. At the same time, as we will show in what follows, the effect is connected with the fact that W^0 and W^1 are different; the magnetoresistance is negative for

$$\eta = W^1/W^0 < 1. \tag{22}$$

The difference between W^0 and W^1 is due to the fact that a transition with spin flip requires participation of an additional real magnon, which carries an uncompensated spin. It is easy to show that the energy of this magnon is $\hbar\Omega_m \sim \max(\hbar\Omega, T)$. Because we have $\hbar\Omega_m \ll J$, the magnon turns out to be long-wavelength, and the corresponding phase volume is small; this means η is small with respect to the parameter of $\hbar\Omega_m/J$.

Thus, by substituting Eqs. (16), (18), (19), (20), (22) into Eq. (17), we obtain

$$W_{ij}(\mathbf{A}_i, \mathbf{A}_j) = w^0 \exp\{-\xi^{sp}(r_{ij}) - (\lambda|\varepsilon_j-\varepsilon_i|+\varepsilon_j-\varepsilon_i)/2T\}\,\Phi(\mathbf{A}_i, \mathbf{A}_j), \tag{23}$$

$$\Phi(A_i, A_j) = \mathrm{ch}^{-1}\left(\frac{A_i}{2T}\right)\left\{(1+\eta)\,\mathrm{ch}\left[(1+\lambda_{ij})\frac{A_j}{4T}\right]\mathrm{ch}\left[(1+\lambda_{ij})\frac{A_i}{4T}\right] + (1-\eta)\,\mathrm{sh}\left[(1+\lambda_{ji})\frac{A_j}{4T}\right]\mathrm{sh}\left[(1+\lambda_{ij})\frac{A_i}{4T}\right]\cos\chi_{ij}\right\}, \tag{24}$$

where $\lambda_{ij} = \lambda$ sign $(\varepsilon_j - \varepsilon_i)$ and W^0 is the coefficient multiplying the exponential. In deriving Eq. (24) we have assumed that the molecular field A (~ 100 K) is smaller than the width of the Mott band. This is valid for $T > 10$ K.

Our next step ought to be averaging Eq. (24) with respect to $\mathbf{n}$. Let us do this within mean-field theory, substituting into Eq. (10) the average antiferromagnetism vector $\mathbf{M}_\alpha$. In this approximation the averaging over $\mathbf{n}$ reduces to replacing the fluctuating molecular field $\mathbf{A}_i$ in Eq. (24) by

$$\langle \mathbf{A}_i \rangle = \omega[\mathbf{M}_{\alpha_i}(\mathbf{a}+\nu_i\mathbf{c})],$$

where α_i is the parity of the layer in which the ith impurity is found. We will assume that the anisotropy parameter (D) and the interplanar exchange (I) correspond to those presented in Ref. 2; this implies that we should consider the following magnetic phases: AF^b, F^b, SF_2^c, SF_1^c, and F^c (see Fig. 3 of Sec. 2). By direct calculation it is easy to verify that for these phases $|\langle \mathbf{A}_i \rangle| = A$ does not depend either on ν_i or on α_i, i.e., it is the same for all acceptors:

$$A = \begin{cases} \omega M, & \mathbf{H}\|\mathbf{b}, \\ \omega M(1+\sin^2\xi)^{1/2}, & (\mathbf{H}\|\mathbf{c}), \end{cases} \tag{25}$$

where $\xi = \xi_{(+)} = \xi_{(-)}$ (see the table and Fig. 6). Then we have

$$\langle \Phi(\mathbf{A}_i, \mathbf{A}_j) \rangle^{mf} = \mathrm{ch}^{-1}\left(\frac{A}{2T}\right)\left\{(1+\eta)\,\mathrm{ch}\left[(1+\lambda)\frac{A}{4T}\right]\mathrm{ch}\left[(1-\lambda)\frac{A}{4T}\right] + (1-\eta)\,\mathrm{sh}\left[(1+\lambda)\frac{A}{4T}\right]\mathrm{sh}\left[(1-\lambda)\frac{A}{4T}\right]\cos\chi_{ij}\right\}. \tag{26}$$

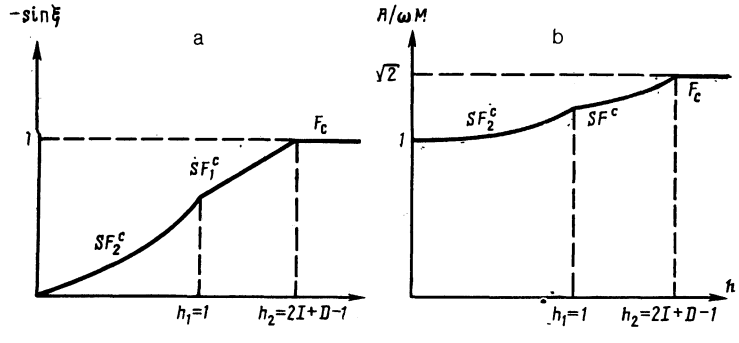

FIG. 6. a—dependence of the angle ξ which determines the direction of the vector $\mathbf{M}$ on the dimensionless magnetic field $h = g\mu_B H/\omega_0^2$ (see Ref. 2), and $\mathbf{H}\|\mathbf{c}$. The kink at the point h_1 corresponds to the transition $SF_2^c \to SF_1^c$, the kink at h_2 is for $SF_1^c \to F^c$. b shows the dependence of the magnitude of the molecular field on h for $\mathbf{H}\|\mathbf{c}$.

This implies that all the dependence of Φ on ij is concentrated in the angle $\cos\chi_{ij} = (\mathbf{A}_i\mathbf{A}_i)/A^2$ (here and in what follows we will omit the angle brackets for $\langle\mathbf{A}_i\rangle$). The expression for $\cos\chi_{ij}$ in the various magnetic phases has the form

$$\cos\chi_{ij}=\begin{cases}1, & (F^b)\\ \alpha_i\alpha_j & (AF^b)\\ \dfrac{(1+\nu_i\nu_j-\alpha_i\alpha_j\nu_i\nu_j)\sin^2\xi+\alpha_i\alpha_j\nu_i\nu_j}{1+\sin^2\xi}, & (SF_1^c)\\ \dfrac{(1+\nu_i\nu_j-\alpha_i\alpha_j)\sin^2\xi+\alpha_i\alpha_j}{1+\sin^2\xi} & (SF_2^c).\end{cases} \tag{27}$$

The case of the F^c phase is a limiting case of the SF_1^c phase for $\sin^2\xi = 1$ and does not require a separate investigation.

As a result, assembling Eqs. (27), (26), (23), and (15), we obtain expressions for the resistance of the Miller–Abrahams network:

$$R_{ij}=B\exp(\xi_{ij}), \tag{28}$$

where

$$B=B_0\Big/\Big[1+\eta\,\mathrm{ch}\Big(\lambda\frac{A}{2T}\Big)\Big/\,\mathrm{ch}\Big(\frac{A}{2T}\Big)\Big],\quad B_0=T/e^2w^0, \tag{29}$$

while the bond function is

$$\xi_{ij}=\xi_{ij}^{(0)}+\delta(\alpha_i\alpha_j,\nu_i\nu_j), \tag{30}$$

$$\xi_{ij}^{(0)}\equiv\xi^{(0)}(\mathbf{r}_i,\varepsilon_i;\mathbf{r}_j,\varepsilon_j)=\xi^{sp}(\mathbf{r}_{ij})+(\lambda|\varepsilon_j-\varepsilon_i|+|\varepsilon_j|+|\varepsilon_i|)/2T \tag{31}$$

and

$$\delta(\alpha_i\alpha_j,\nu_i\nu_j)=f(\cos\chi_{ij}),$$
$$f(x)=\ln\Big\{\frac{2[\mathrm{ch}(A/2T)+\eta\,\mathrm{ch}(\lambda A/2T)]}{[1+\eta+(1-\eta)x]\mathrm{ch}(A/2T)+[1+\eta-(1-\eta)x]\mathrm{ch}(\lambda A/2T)}\Big\}. \tag{32}$$

For the case $\mathbf{H}\|\mathbf{b}$, the angle χ_{ij} does not depend on $\nu_i\nu_j$ (because $\mathbf{M}_\alpha\|\mathbf{c}$) and, therefore, R_{ij} is insensitive to the ordering characteristics of ν_i (see Section 3). For the F^b-phase, we have $\cos\chi_{ij}=1$ and

$$\delta=0, \tag{33}$$

i.e., ξ_{ij} does not depend on $\alpha_i\alpha_j$. For the AF^b phase

$$\delta(\alpha_i\alpha_j,\nu_i\nu_j)=\begin{cases}0, & \alpha_i\alpha_j=+,\\ \delta\equiv f(-1), & \alpha_i\alpha_j=-.\end{cases} \tag{34}$$

For the case $\mathbf{H}\|\mathbf{c}$, the result depends on how the ν_i are ordered; we consider these types of order individually.

For frozen-in disorder

$$\delta(\alpha_i\alpha_j,\nu_i\nu_j)=\begin{cases}0, & \alpha_i\alpha_j=+, & \nu_i\nu_j=+,\\ \delta_1(\delta_3), & \alpha_i\alpha_j=+, & \nu_i\nu_j=-,\\ \delta_2, & \alpha_i\alpha_j=-, & \nu_i\nu_j=+,\\ \delta_3(\delta_1), & \alpha_i\alpha_j=-, & \nu_i\nu_j=-,\end{cases}\qquad SF_1^c\,(SF_2^c) \tag{35}$$

where $\delta_\mu=f(\cos\chi_\mu)$, $\mu=1,2,3$ and

$$\cos\chi_{1,3}=\mp\frac{1-\sin^2\xi}{1+\sin^2\xi},\qquad \cos\chi_2=\frac{3\sin^2\xi-1}{1+\sin^2\xi}. \tag{36}$$

For the case when the ν_i are ordered, we have

$$\delta(\alpha_i\alpha_j,+)=\begin{cases}0, & \alpha_i\alpha_j=+,\\ \delta_2, & \alpha_i\alpha_j=-\end{cases}\qquad SF_1^c, SF_2^c, \tag{37}$$

for uniform order, and

$$\delta(\alpha_i\alpha_j,\alpha_i\alpha_j)=\begin{cases}0, & \alpha_i\alpha_j=+,\\ \delta_3(\delta_1), & \alpha_i\alpha_j=-,\end{cases}\qquad SF_1^c,\ (SF_2^c) \tag{38}$$

for alternating order. For the case of dynamic disorder ($\tau_n\ll\tau_\nu\ll\tau_0$), the average with respect to t in formula (15) implies that Eq. (26) for $\cos\chi_{ij}$, which enters into (32), must be averaged with respect to ν_i and ν_j:

$$\langle\cos\chi_{ij}\rangle_\nu=\begin{cases}\sin^2\xi/(1+\sin^2\xi), & SF_1^c,\\ [(1-\alpha_i\alpha_j)\sin^2\xi+\alpha_i\alpha_j]/(1+\sin^2\xi), & SF_2^c.\end{cases} \tag{39}$$

As a result, the quantity δ retains only its dependence on $\alpha_i\alpha_j$:

$$\delta(\alpha_i\alpha_j)=\bar\delta=f(\sin^2\xi/(1+\sin^2\xi)) \tag{40}$$

for the SF_1^c phase and

$$\delta(\alpha_i\alpha_j)=\begin{cases}\bar\delta_1=f(1/(1+\sin^2\xi)), & \alpha_i\alpha_j=+,\\ \bar\delta_2=f((2\sin^2\xi-1)/(1+\sin^2\xi)), & \alpha_i\alpha_j=-\end{cases} \tag{41}$$

for the SF_2^c phase.

5. GENERALIZED PERCOLATION THEORY

In the preceding section we calculated the resistance of a Miller–Abrahams network whose nodes represent the acceptors. For this problem, as in the problem of hopping conductivity in normal doped semiconductors,[4] the scatter in resistance is exponentially large and the methods of percolation theory can be applied. However, for our problem this method must be modified because the bond functions ξ_{ij} [see Eq. (30)] depend not only on the continuously distributed random quantities $(\mathbf{r}_i,\varepsilon_i)$, but also on the discrete quantities (α_i,ν_i). The resistive networks in question can be divided into three groups:

1. ξ_{ij} does not depend on $\alpha_i\alpha_j$ or $\nu_i\nu_j$. To this group belong the F^b phase for any type of ordering of the ν and the dynamic disorder case for the SF_1^c phase.

2. ξ_{ij} depends on $\alpha_i\alpha_j$ but not on $\nu_i\nu_j$: the AF^b phase for any type of ν ordering, the SF_2^c phase for the case of dynamic disorder, and the SF_1^c and SF_2^c phases for the ordered cases (uniform or alternating) all belong to this group.

3. ξ_{ij} depends both on $\alpha_i\alpha_j$ and on $\nu_i\nu_j$: the SF_1^c and SF_2^c phases (frozen-in disorder) belong to this group.

Let us consider these types of networks individually.

1. For this case we can apply the standard percolation method. In order to determine the threshold for percolation ξ_c, it is necessary to calculate the average number of sites in the four-dimensional space (r_i,ε_i) that are linked to a given site based on the criterion for linking $\xi_{ij}<\xi_c$. This number must then be set equal to a certain constant c of the dimen-

sionless percolation problem:

$$^1/_4 gTa_\parallel{}^2 a_\perp \xi_c{}^4 = c, \tag{42}$$

where g is the density of states at the Fermi level.

The constant c depends on the structure of the dimensionless percolation problem, i.e., on the value of λ [see (21)] and the functional form of $\xi^{sp}(r_{ij})$. Including the temperature dependence of λ in the theory of polaron hopping conduction leads to a weak deviation from the Mott law.[33] Trials based on numerical calculations have shown that the form of the surface $\xi_{ij} = \text{const}$ in (r_i, ε_i) space has almost no effect on the constant c (see Ref. 4), and we will neglect this effect in what follows.

From this we see that the percolation threshold satisfies

$$\xi_c = (T_0/T)^{1/4} \equiv \xi_0, \tag{43}$$

where $T_0 = 4c/ga_\parallel^2 a_\perp$.

2. The sites are grouped into two different classes ($\alpha_i = +$) and ($\alpha_i = -$) (Fig. 7a), and sites belonging to each of the classes are randomly distributed in space. The linking function for sites from one class ($\alpha_i \alpha_j = +$) is $\xi_{ij}^{(0)}$, while the linking function for sites in the other class ($\alpha_i \alpha_j = -$) is $\xi_{ij} + \delta$. The percolation threshold ξ_c in this generalized percolation problem is a function of the quantity δ: $\xi_c = \xi_c(\delta)$. For $\delta = 0$, all the sites are equivalent (i.e., the classes merge) and the problem reduces to the previous one: $\xi_c^{(0)} = \xi_0$. In order to determine ξ_c for finite δ, we substitute into Eq. (42) the total number of sites (from both classes) that satisfy the criterion for linking to a given (arbitrarily chosen) site:

$$^1/_4 (g/2) T a_\parallel{}^2 a_\perp [\xi_c{}^4 + (\xi_c - \delta)^4 \theta(\xi_c - \delta)] = c, \tag{44}$$

where $\theta(x)$ is the Heaviside function. Neglecting the dependence of c on the shape of the region, we rewrite Eq. (44) in the form

$$\xi_c{}^4 + (\xi_c - \delta)^4 \theta(\xi_c - \delta) = 2\xi_0{}^4, \tag{45}$$

from which the percolation threshold (see Fig. 7c) is

$$\xi_c(\delta) = \begin{cases} \dfrac{\delta}{2} + \left[\left(\dfrac{\delta^4}{2} + \xi_0{}^4\right)^{1/2} - \dfrac{3}{4}\delta^2\right]^{1/2}, & \delta < 2^{1/4}\xi_0, \\ 2^{1/4}\xi_0, & \delta > 2^{1/4}\xi_0. \end{cases} \tag{46}$$

For $\delta > 2^{1/4}\xi_0$, all the bonds between sites belonging to different classes are broken: percolation takes place along each of the classes independently and the percolation threshold corresponds to the density of states being decreased by half.

For $\delta \ll \xi_0$ we have

$$\xi_c(\delta) \approx \xi_0 + \delta/2. \tag{47}$$

3. All the sites of the network are divided into four equal classes: ($\alpha_i = +$, $\nu_i = +$), ($+ -$), ($- +$), and ($- -$). The structure of the links between classes is illustrated in Fig. 7b.

By reasoning analogous to that used previously, we are led to an equation for the percolation threshold $\xi_c = \xi_c(\delta_1, \delta_2, \delta_3)$:

$$\xi_c{}^4 + \sum_{\mu=1}^{3} (\xi_c - \delta_\mu)^4 \theta(\xi_c - \delta_\mu) = 4\xi_0{}^4. \tag{48}$$

For the case that is of most interest to us, the solution to Eq. (48) has the form

$$\xi_c = \xi_0 + {}^1/_4 \sum_{\mu=1}^{3} \delta_\mu, \quad \delta_\mu \ll \xi_0. \tag{49}$$

Taking up where we left off, we present expressions for the resistivity of a sample in the various magnetic phases (we will assume $\delta \ll \xi_0$; however, in this case the condition $\delta \gtrsim 1$ is allowed, because $\xi_0 \sim 10$ for $T \sim 100$ K):

$$R = B \exp(\xi_0), \quad F^b, \tag{50}$$

$$R = B \exp(\xi_0 + \delta/2), \quad AF^b \tag{51}$$

for all types of ordering of ν, and

$$R = B \exp\left(\xi_0 + {}^1/_4 \sum_{\mu=1}^{3} \delta_\mu\right), \quad SF_1{}^c, \quad SF_2{}^c \tag{52}$$

for the case of frozen-in disorder. In the SF_1^c and SF_2^c phases the expressions for R are the same because of the symmetry of $\xi_c(\delta_\mu)$ relative to the permutations δ_μ [see Eq. (48)]. Finally,

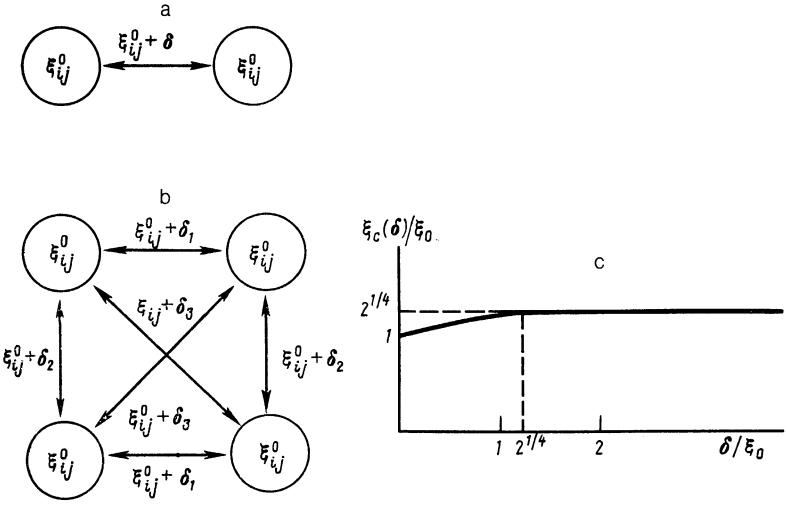

FIG. 7. Schematic illustration of the generalized percolation problem. The circles show the classes of the sites; shown in the circles are the coupling functions within the classes. The connecting function between sites of different classes are written near the arrows that connect the corresponding classes: a—the case of two classes, b—the case of four classes, c—the dependence of the percolation threshold ξ_c on the value of δ for the case of two classes.

$$R=B\exp(\xi_0+\delta),\quad SF_1^c, \tag{53}$$

$$R=B\exp[\xi_0+{}^1/_2(\delta_1+\delta_2)],\quad SF_2^c \tag{54}$$

for dynamic disorder,

$$R=B\exp(\xi_0+\delta_2/2),\quad SF_1^c,\quad SF_2^c \tag{55}$$

for uniform disorder, and

$$R=B\exp(\xi_0+\delta_1/2),\quad SF_1^c, \tag{56}$$

$$R=B\exp(\xi_0+\delta_3/2),\quad SF_2^c \tag{57}$$

for alternating order.

The coefficient B in Eqs. (50)–(57) differs from that of Eq. (29) because of the preexponential factors of the theory of percolation. However, for $\delta \ll \xi_0$ this factor is the same for all the magnetic phases, independent of the magnetic field, and its role reduces to renormalizing the quantity B_0.

6. DISCUSSION AND COMPARISON WITH EXPERIMENT

Here we will discuss effects that may be observable if the spin mechanism for magnetoresistance discussed in this paper is valid, and look for qualitative agreement between our results and the data of Refs. 1 and 2 concerning magnetoresistance in La_2CuO_4.

In what follows we limit ourselves to the case $T > T^*$, for which $\lambda = 0$. Allowing for $\lambda \neq 0$ does not lead to qualitative changes at lower temperatures, and we will not evaluate the corresponding very involved expressions. In all cases the quantity T^* [Eq. (21)] must be considerably smaller than 50 K, because $\hbar\Omega \sim 100$ K holds (see Ref. 18) while $\ln(W/\Delta) > 1$.

Let us begin with the case $\mathbf{H}\|\mathbf{b}$. The resistance in a field $H < H_c = J_\perp J/g\mu_B\omega_0$, i.e., in the AF^b phase, does not depend on the field and equals

$$R(H)=R(0)=B_0(T)\operatorname{ch}\left(\frac{\omega M}{2T}\right)\left\{\left[1+\eta\operatorname{ch}\left(\frac{\omega M}{2T}\right)\right]\times\left[\eta+\operatorname{ch}\left(\frac{\omega M}{2T}\right)\right]\right\}^{-1/2}, \tag{58}$$

where $B_0(T) = B\exp[T/T_0)^{1/4}]$. In agreement with the experimental curve shown in Fig. 1a, the resistance undergoes a jump at the point $H = H_c$ and for $H > H_c$, i.e., in the F^b phase, it once again is independent of H:

$$R(H)=R(\infty)=B_0(T)\operatorname{ch}\left(\frac{\omega M}{2T}\right)\left[\eta+\operatorname{ch}\left(\frac{\omega M}{2T}\right)\right]^{-1}. \tag{59}$$

The magnitude of the relative jump in resistance is

$$\Delta R/R=[R(0)-R(\infty)]/R(\infty)=\left\{\left[\operatorname{ch}\left(\frac{\omega M}{2T}\right)+\eta\right]\Big/\left[1+\eta\operatorname{ch}\left(\frac{\omega M}{2T}\right)\right]\right\}^{1/2}-1. \tag{60}$$

Near the Néel temperature, where $M(T) \ll 1$, we have

$$\Delta R/R=\frac{1-\eta}{1+\eta}\frac{\omega^2}{16T^2}M^2(T). \tag{61}$$

The experimental curve (Fig. 1c) is qualitatively described by Eq. (60) for $\omega \sim 100$ K (with regard to the steep dropoff see below). The proportionality of $\Delta R/R$ and $M^2(T)$ predicted by Eq. (61) is also in qualitative agreement with Fig. 1c near T_N.

In Ref. 3 the authors found a jump in the resistance that was considerably smaller than in Refs. 1 and 2 (on the order of 10%) and was strongly washed out; in addition, it was correlated with jumps in the total magnetic moment. Apparently this is explained by the large number of impurities and by the inhomogeneity of the samples investigated in Ref. 3.

Comparing our results with the experimental data of Ref. 1 for $\mathbf{H}\|\mathbf{b}$ allows us to exclude the configurations of acceptors of the form shown in Fig. 3e, because for these configurations all the χ_{ij} vanish, and we have $A = 0$ for $H < H_c$ and $A = 2\omega M(T)$ for $H > H_c$. The magnetoresistance in this case should be determined only by the coefficient factor B [Eq. (29)] and would be positive, not negative.

As for the various types of ordering of ν_i (i.e., the **c** component of the local rhombohedral distortion), the data of Ref. 1 do not allow us to choose between them because for $\mathbf{H}\|\mathbf{b}$ the antiferromagnetic moments $\mathbf{M}_\alpha$ are parallel to **c**.

In a field $\mathbf{H}\perp\mathbf{b}$ the magnetoresistance depends strongly on the type of ordering of the ν_i. However the latter is clearly determined by the quality of the crystal and the conditions under which it was annealed. Because the oxygen diffusion coefficient is large,[16] the type of ordering of the ν_i can be determined by the kinetics of this diffusion and possibly may change even from measurement to measurement, if the sample is subject to heating between measurements. Therefore, in the previous sections we have developed a theory that is applicable to the various types of ordering of the ν_i:

(a) frozen-in disorder;
(b) uniform order;
(c) alternating order;
(d) dynamic disorder.

In addition, in contrast to the case $\mathbf{H}\|\mathbf{b}$ the magnetoresistance is sensitive to whether or not **a**–**c** domains are present in the sample.

Let us discuss to what extent the theory proposed here can explain the results of the experiments of Ref. 2 in fields $\mathbf{H}\|\mathbf{a}, \mathbf{c}$. We first turn our attention to three important qualitative experimental facts: first of all, the magnetoresistance is always negative and is a monotonic function of field. Secondly, for magnetic phase transitions the dependence of the resistance on field has kinks; however, it never has jumps. Thirdly, in certain cases, although not in all (see Ref. 2), the total change in the resistance $\Delta R/R = [R(0) - R(\infty)]/R(\infty)$ is the same in magnitude and temperature dependence for $\mathbf{H}\|\mathbf{b}$ and $\mathbf{H}\perp\mathbf{b}$.

Let us first consider field orientations $\mathbf{H}\|\mathbf{c}$. The magnetoresistance described by Eqs. (52)–(57) is negative for all the cases (a)–(d). Furthermore, the magnetoresistance has kinks in all cases but does not have a jump for $H = H_2 = 2(J_\perp + \Delta)J/g\mu_B\omega_0 - \omega_0/g\mu_B$, i.e., for $SF_1^c \to F^c$ transitions, because this transition is second order and is not accompanied by jumps in the values of the antiferromagnetic moments $\mathbf{M}_\alpha$.

The situation is otherwise for the $SF_2^c \to SF_1^c$ transition in a field $H_1 = \omega_0/g\mu_B$, for which a discontinuous reorientation of the $\mathbf{M}_\alpha$ occurs from the **bc** plane to the **ab** plane. Associated with this transition is a reorientation of the molecular fields $\mathbf{A}_i$ [see Eqs. (10), (11)], leading in general to a jump in the angle χ_{ij} and consequently to a jump in the resistance. This jump does in fact occur for the (c) and (d) types of ordering of the ν_i; however, it is absent for the cases (a) and (b). The absence of a jump is due to the symmetries

of the classes of corresponding percolation problems with respect to a reflection which interchanges the planes **ba** and **bc**. If we assume that the jump in $R(H)$ at a field H_1 takes place anyway [i.e., cases (c) or (d) are realized], but is smeared out because of some mechanism, then this same mechanism would clearly have to smear out the jump in the field H_c as well for $\mathbf{H}\|\mathbf{b}$. Because this latter type of smearing is not observed experimentally, the absence of a jump in $R(H)$ for $\mathbf{H}\|\mathbf{c}$ allows us to exclude the types of order (c) and (d) (at any rate, for the samples investigated in Ref. 2).

In order to make a choice between the remaining types of ordering let us consider the quantity $R(\infty)$:

$$R(\infty)=\left(\frac{2}{1+\eta}\right)^{1/2}B_0(T)\left\{\left[\eta+\operatorname{ch}\left(\frac{\omega M}{\sqrt{2}T}\right)\right]\times\left[\operatorname{ch}\left(\frac{\omega M}{\sqrt{2}T}\right)+1\right]\right\}^{-1/2}\operatorname{ch}\left(\frac{\omega M}{\sqrt{2}T}\right), \tag{62a}$$

$$R(\infty)=B_0(T)\operatorname{ch}\left(\frac{\omega M}{\sqrt{2}T}\right)\Big/\left[\eta+\operatorname{ch}\left(\frac{\omega M}{\sqrt{2}T}\right)\right] \tag{62b}$$

for the types (a) and (b), respectively. For finite η both quantities differ from Eq. (59) for $\mathbf{H}\|\mathbf{b}$. However, the quantity η is most likely small (see Section 4), and in this case Eq. (62b) coincides with Eq. (59), while Eq. (62a) differs from it as before (by roughly a factor of $\sqrt{2}$). From this we see that the overall change in resistance $\Delta R/R$ is universal only for ordering of type (b) and small η. Therefore, we think that in those measurements which recorded identical changes in the resistance for $\mathbf{H}\|\mathbf{b}$ and $\mathbf{H}\perp\mathbf{b}$, the quantities ν_i were type-(b) orderings and the field was oriented along **c**. Then the dependence of the resistance on field (for $\eta=0$) takes the form

$$R=B_0(T)\,(1+\sin^2\xi)^{1/2}\left\{2\sin^2\xi+\left[\cos^2\xi/\operatorname{ch}\left[\frac{\omega M}{2T}(1+\sin^2\xi)^{1/2}\right]\right]\right\}^{-1/2}, \tag{63}$$

where $\sin\xi$ is a function of magnetic field (see Fig. 6a and the table).

The resistance calculated by using this formula agrees with the experimental curves in Fig. 1b. In a field H_1 there is no jump in the resistance R, and the only kink present is the one connected with the kink in ξ. Above H_2 the angle ξ is constant and R saturates.

The results presented here are valid for a single-domain sample in a field $\mathbf{H}\|\mathbf{c}$. However, the majority of samples investigated in Ref. 2 were multidomain: a portion of the domains corresponded to the orientation $\mathbf{H}\|\mathbf{c}$ while another portion corresponded to $\mathbf{H}\|\mathbf{a}$. In the orientation $\mathbf{H}\|\mathbf{a}$ the magnetoresistance must be absent, i.e., $R(H)\equiv R(0)$, because the antiferromagnetic moments are not sensitive to the field $\mathbf{H}\|\mathbf{a}$ (see Section 2). From this we see that the resistance of a multidomain sample will be a certain average of the resistances Eq. (63) for domains with $\mathbf{H}\|\mathbf{c}$ and $R(0)$ for domains with $\mathbf{H}\|\mathbf{a}$. The method of averaging depends on the specific geometry of the domains; in any case, the field dependence of the effective resistance will not be qualitatively different from Eq. (63). At the same time the total jump in $\Delta R/R$ must decrease somewhat. On the other hand, in a field $\mathbf{H}\|\mathbf{b}$ the multidomain character is not present; therefore, in our view, we should not expect any universality in the overall variation in the resistance of a multidomain sample.

The results presented above were obtained in the mean-field approximation. Let us now discuss qualitatively how fluctuations in the antiferromagnetism vector **n** should affect the magnetoresistance. Strictly speaking, in taking into account fluctuations it is not really legitimate to use expression (17) for the transition probability from the i-th to the j-th acceptor, because in this case the latter becomes a function of **n** along all paths for tunneling. Nevertheless, in a number of cases (for example, for tunneling without spin–flip) Eq. (17) remains valid. We have assumed that taking into account fluctuations should in all cases lead to a decrease in the magnetoresistance compared to the mean field result. The easiest way to verify this is to assume that fluctuations of $\mathbf{n}_i$ and $\mathbf{n}_j$ are uncorrelated. This condition is valid when the mean hopping length in the direction perpendicular to the layers is larger than the magnetic correlation length in this same direction, and holds everywhere except within a narrow region around T_N.

In neutron scattering experiments[34] (which, unfortunately, were not carried out on the samples used in Refs. 1 and 2) a sharp drop in $M(T)$ has been observed for $T\lesssim 25$ K. It is possible that this sharp falloff is connected with the enhancement of the magnetic fluctuations at low temperature caused by the effect of frustrating magnetic impurities.[35] In this case it is natural to assume that both of these falloffs are due to the same fluctuation mechanism. Phenomenologically the falloff in $\Delta R/R$ can be explained by the falloff in $M(T)$ even within the mean-field framework. Thus, we can assume that the mean-field results presented above are qualitatively valid in practice over the entire temperature range.

Thus, the spin mechanism allows us to explain qualitatively all of the features of the magnetoresistance of insulating La_2CuO_4 observed in the experiments of Refs. 1 and 2. However, a quantitative comparison is hindered by the following facts. First of all, as shown in Refs. 2 and 16, the conductivity for $T\gtrsim 50$ K is dominated by a mechanism which is not described by the Mott law; apparently, it is not a hopping mechanism and does not give any contribution to the magnetoresistance. Including this mechanism should lead to a decrease in the magnitude of $\Delta R/R$ for $T\gtrsim 50$ K. For a quantitative comparison of theory with experiment it is necessary to be able to distinguish the hopping contribution to R. Secondly, for $\mathbf{H}\perp\mathbf{b}$ the only data that is admissible for a direct comparison with theory is data obtained on single-domain samples.

In conclusion, we will discuss the possibility of experimental verification of assumptions 1 and 2 concerning the structure of the acceptor state proposed in the Introduction. The identification of vibronic structure in the optical spectra[30] is very difficult because, on one hand, it requires high-purity material and, on the other hand, detailed knowledge of the constants of the vibronic Hamiltonian. However, it is possible to identify transitions between spin sublevels of the acceptors because, according to our theory, their frequency equals the magnitude of the molecular field A and depends on the field H (see Fig. 6b) in agreement with Eq. (25) and the table. This dependence is detectable in the field $\mathbf{H}\|\mathbf{c}$ (in the field $\mathbf{H}\|\mathbf{b}$ we have $A(H)\equiv A(0)\sim 100$ K); the frequency of the transition increases monotonically in a field $H<H_2$ and undergoes a kink in the fields H_1 and H_2, and for $H>H_2$ we have $A(H)\equiv A(H_2)=\sqrt{2}A(0)$. Optical observation of

such a magnetic-field-dependent transition would be proof of the two-component local enhancement of the rhombohedral distortion and would allow us to determine its magnitude. In addition, this would permit an independent identification of the magnetic phase transitions for **H**||**c**. In multidomain samples, in addition to lines with frequency $A(H)$ (from **c**-oriented domains), we should also observe a line with frequency $A(0)$ (from the **a**-domains); this would appear as a splitting of the magnetic field line.

Certain results of this paper touching only on the case **H**||**b** were previously published in a brief communication.[36]

We are grateful to Tineke Thio, Mark Kastner, Robert Birgenau, and Norris Preyer for discussing the experimental situation and also to S. A. Brazovskii, Bertrand Halperin, M. E. Reich, D. E. Khmel'nitskii, E. G. Tsitsishvili, and V. I. Shklovskii for discussing the work and for useful comments. We also acknowledge T. Yu. Gnedovskii for his help and support at all stages of this work.

[1] T. Thio, T. R. Thurston, N. W. Preyer *et al.*, Phys. Rev. B **38**, 905 (1988).
[2] T. Thio, C. Y. Chen, B. S. Freer *et al.*, Phys. Rev. B **41**, 231 (1990).
[3] S. -W. Cheong, Z. Fisk, J. O. Willis *et al.*, Solid State Commun. **65**, 111 (1988).
[4] B. I. Shklovskii and A. F. Éfros, *Electronic Properties of Doped Semiconductors*, Springer, New York, 1984.
[5] G. Appel, in Yu. A. Firsov ed., *Polarons*, Nauka, Moscow, 1975.
[6] B. Z. Spivak, Zh. Eksp. Teor. Fiz. **87**, 1371 (1984) [Sov. Phys. JETP **60**, 787 (1984)].
[7] J. G. Bednorz and K. A. Müller, Z. Phys. B **64**, 189 (1986).
[8] J. G. Birgenau and G. Shirane, *Physical Properties of High-Temperature Superconductors*. Ginsberg ed., Singapore: World Scientific, 1989.
[9] M. A. Kastner, R. J. Birgenau, T. R. Thurston *et al.*, Phys. Rev. B **38**, 6636 (1988).
[10] A. S. Borovik-Romanov, A. I. Buzdin, N. M. Kreines, and S. S. Krotov, Pis'ma Zh. Eksp. Teor. Fiz. **47**, 600 (1988) [JETP Lett. **47**, 697 (1988)].
[11] S. S. Krotov and R. M. Farzetdinov, Superconductivity **2**, 60 (1989).
[12] A. I. Vazhan, V. N. Bevz, V. A. Merzhanov *et al.*, Pis'ma Zh. Eksp. Teor. Fiz. **48**, 21 (1988) [JETP Lett. **48**, 21 (1988)].
[13] I. Dzyaloshinskii, J. Phys. Chem. Solids **4**, 241 (1958).
[14] T. Moriya, Phys. Rev. **120**, 91 (1960).
[15] M. A. Kastner, R. J. Birgenau, C. Y. Chen *et al.*, Phys. Rev. B **37**, 111 (1988).
[16] N. W. Preyer, R. J. Birgenau, C. Y. Chen *et al.*, Phys. Rev. B **39**, 11563 (1989).
[17] N. F. Mott and E. Davis, *Electronic Processes in Noncrystalline Materials* 2nd ed., Clarendon, Oxford, 1974.
[18] A. O. Gogolin and A. S. Noselevich, Pis'ma Zh. Eksp. Teor. Fiz. **50**, 468 (1989) [JETP Lett. **50**, 502 (1989)].
[19] Y. Nagaoka, Phys. Rev. **147**, 392 (1966).
[20] A. Aharony, R. J. Birgenau, A. Conglio *et al.*, Phys. Rev. Lett. **60**, 1130 (1988).
[21] L. I. Glazman and A. S. Noselevich, Pis'ma Zh. Eksp. Teor. Fiz. **47**, 464 (1988) [JETP Lett. **47**, 547 (1988)].
[22] D. C. Jonston, S. K. Shinha, A. J. Jacobson, and J. M. Newsam, Physica C **153–155**, 572 (1988).
[23] J. W. Rogers, N. D. Shinn, J. E. Schriber *et al.*, Phys. Rev. B **38**, 5021 (1988).
[24] C. Y. Chen, N. W. Preyer, P. J. Picone *et al.*, Phys. Rev. Lett. **63**, 2307 (1989).
[25] V. L. Pokrovsky and G. V. Uimin, Physica C **160**, 323 (1989).
[26] V. J. Emery, Phys. Rev. Lett. **58**, 2794 (1987).
[27] A. F. Barabanov, L. A. Maksimov, and G. V. Uimin, Pis'ma Zh. Eksp. Teor. Fiz. **47**, 532 (1988) [JETP Lett. **47**, 622 (1988)].
[28] E. Lieb and A. Mattis, Phys. Rev. **125**, 164 (1962).
[29] E. L. Nagaev, *Physics of Magnetic Semiconductors*, Mir, Moscow, 1979.
[30] I. B. Bersuker, *The Jahn–Teller Effect and Vibronic Interactions in Modern Chemistry*, Plenum, New York (1983).
[31] T. R. Thurston, R. J. Birgenau, D. R. Gabbe *et al.*, Phys. Rev. B **39**, 4327 (532).
[32] H. Sher and T. Holstein, Phil. Mag. B **44**, 343 (1981).
[33] S. D. Baranovskii and V. G. Karpov, Fiz. Tekh. Poluprovodn. **20**, 1811 (1986) [Sov. Phys. Semicond. **20**, 1137 (1986)].
[34] Y. Endoh, K. Yamada, R. J. Birgenau *et al.*, Phys. Rev. B **37**, 7443 (1988).
[35] L. I. Glazman and A. S. Noselevich, Pis'ma Zh. Eksp. Teor. Fiz. **49**, 503 (1989) [JETP Lett. **49**, 579 (1989)].
[36] A. O. Gogolin and A. S. Ioselevich, Pis'ma Zh. Eksp. Teor. Fiz. **51**, 154 (1990) [JETP Lett. **51**, 174 (1990)].

Translated by Frank J. Crowne